

# Ultraspherical wavelets approach to solve nonlinear fractional HIRES problem with application in Chemical Kinetics

<sup>1\*</sup>Ashish Rayal, <sup>2</sup>Jasmeet Kaur, <sup>3</sup>Vikash Verma, <sup>4</sup>Priya Dogra

Communicated by Jagan Mohan Jonnalagadda

MSC 2010 Classifications: Primary 41A10, 65D25; Secondary 65D15, 65T60.

Keywords and phrases: Fractional HIRES problem, Ultraspherical Wavelets, Function approximation, Collocation nodes, Errors.

*The authors would like to thank the reviewers and editor for their constructive comments and valuable suggestions that improved the quality of our paper.*

**Corresponding Author: Ashish Rayal**

**Abstract** Simulating the dynamics of complex systems of initial value problems in chemistry is becoming increasingly routine with increasing computer power. In the realm of chemical kinetics, the High Irradiance Responses (HIRES) of Photomorphogenesis from Plant Physiology stands as a significant challenge due to its intricate nature and the demand for precise numerical solutions. Therefore, this study demonstrates the use of the ultraspherical wavelets basis to solve the HIRES problem of fractional order. The utilization of ultraspherical wavelets allows for the representation of functions with high precision, while the Caputo fractional derivative provides a comprehensive framework for describing the non-local and memory-dependent aspects inherent in chemical kinetics. The proposed approach is employed to numerically simulate a system of stiff non-linear differential equations and has calculated several errors for nonlinear fractional HIRES problem. Furthermore, the residual error analysis for this model is also computed. With the use of wavelet transform, the nonlinear HIRES problem is solved, aiding in the understanding of chemical reactions and their true behaviors. The effectiveness of the mentioned approach is demonstrated by numerical simulation in terms of tables and figures, showcasing its potential to advance the field of chemical kinetics modeling and simulation.

## 1 Introduction

In recent years, fractional calculus [1, 2], a branch of mathematical analysis has garnered significant attention due to its profound implications across various scientific disciplines including chemical kinetics. Traditional calculus deals with integer-order derivatives and integrals, which describe instantaneous rates of change and cumulative effects, respectively. Many natural phenomena exhibit non-local or memory-dependent behaviors that cannot be adequately described using integer-order calculus [2]. Fractional calculus generalizes differentiation and integration to non-integer orders, enabling the modeling of complex dynamics that involve fractional derivatives and integrals. Among others, one of the most widely employed operators is the Caputo fractional derivative [3]. It is a powerful mathematical tool that has found widespread applications in various areas. One of the primary benefits of the Caputo fractional derivative, compared to other fractional definitions is its compatibility with the traditional initial conditions used in the study of differential equations. Another important advantage is its improved numerical stability, particularly when dealing with noisy or irregular data. The Caputo definition tends to be more robust to these challenges compared to other fractional derivative definitions, which can be more susceptible to numerical instabilities. With these important remarks, the Caputo definitions have been employed in the simulations of models with physical importance. Fractional differential equations have crucial roles in several disciplines. Due to their great importance, they have been investigated by many researchers. For instance, Abd-Elhameed et al. [4, 5] applied a Chebyshev approach to simulate the Sinh-Gordon equation and fractional Rayleigh-

Stokes problem. In [6], Alharbi et al. implemented a shifted Fibonacci polynomials approach to solve the fractional Burgers equation. Recently, Abd-Elhameed et al. [7] presented an effective Fibonacci collocation scheme for solving the Fitzhugh-Nagumo equation. For more details, see [8, 9, 10, 11, 12, 13] and the references therein.

Several physical models lead to the formation of stiff ordinary differential equations (ODEs). These equations typically arise in biochemistry, control theory, fluid dynamics, chemical kinetics, etc. HIRES problem is one of the most important topics in chemical kinetics [14, 15] that is related to the influence of plant morphogenesis by light. The challenge of addressing HIRES problem in photomorphogenesis, wherein plants undergo physiological and developmental changes in response to high levels of light irradiation, represents a complex yet crucial aspect of understanding plant biology and optimizing agricultural practices [16, 17]. The significance of fractional calculus in chemical kinetics lies in its ability to provide more accurate and realistic representations of kinetic processes. Traditional methods of solving chemical kinetics equations often assume instantaneous reactions and spatial homogeneity, neglecting the effects of spatial dispersion, memory, and long-range interactions. However, many real-world chemical reactions exhibit complex dynamics influenced by factors such as diffusion, heterogeneity, and non-Markovian behavior. By incorporating fractional derivatives and integrals into kinetic models, researchers can capture these intricate dynamics more effectively.

The chemical reaction process in HIRES problem has been formulated as a stiff system of eight non-linear ODEs [18] which is expressed in the fractional form as

$$\begin{aligned}
 D_{0,\rho}^\lambda Y_1(\rho) &= -\beta_1 Y_1(\rho) + \beta_2 Y_2(\rho) + \beta_3 Y_3(\rho) + \beta_4, \\
 D_{0,\rho}^\lambda Y_2(\rho) &= \beta_1 Y_1(\rho) - \beta_5 Y_2(\rho), \\
 D_{0,\rho}^\lambda Y_3(\rho) &= -\beta_6 Y_3(\rho) + \beta_2 Y_4(\rho) + \beta_7 Y_5(\rho), \\
 D_{0,\rho}^\lambda Y_4(\rho) &= \beta_3 Y_2(\rho) + \beta_8 Y_3(\rho) - \beta_9 Y_4(\rho), \\
 D_{0,\rho}^\lambda Y_5(\rho) &= -\beta_{10} Y_5(\rho) + \beta_2 Y_6(\rho) + \beta_2 Y_7(\rho), \\
 D_{0,\rho}^\lambda Y_6(\rho) &= -\beta_{11} Y_6(\rho) Y_8(\rho) + \beta_{12} Y_4(\rho) + \beta_8 Y_5(\rho) - \beta_2 Y_6(\rho) + \beta_{12} Y_7(\rho), \\
 D_{0,\rho}^\lambda Y_7(\rho) &= \beta_{11} Y_6(\rho) Y_8(\rho) - \beta_{13} Y_7(\rho), \\
 D_{0,\rho}^\lambda Y_8(\rho) &= -\beta_{11} Y_6(\rho) Y_8(\rho) + \beta_{13} Y_7(\rho),
 \end{aligned} \tag{1.1}$$

with initial values

$$(Y_1(0), Y_2(0), Y_3(0), Y_4(0), Y_5(0), Y_6(0), Y_7(0), Y_8(0)) = (a_1, a_2, a_3, a_4, a_5, a_6, a_7, a_8). \tag{1.2}$$

Here,  $D_{0,\rho}^\lambda$  denotes the fractional Caputo derivative of order  $\lambda \in (0, 1]$ ,  $\beta_s$  is a kinetic constant for  $s = 1, 2, \dots, 13$  and  $a_j$  is a constant value for  $j = 1, 2, \dots, 8$ .

In order to demonstrate convergence in stiff chemical kinetics issues, Amat et al. [18] described variational approach for numerical simulation of stiff differential equations. In [19], Soomro et al. proposed a 3-point variable step block hybrid technique that makes use of Lagrange polynomials. Efficient time-stepping strategy for analyzing turbulent reactive flows under stiff chemistry is developed by Wu et al. [20]. This technique may prove useful in comprehending intricate chemical processes. Skwame et al. [21] shown the potential of hybrid approaches in resolving chemical kinetics difficulties by creating an equidistant one-step block hybrid technique that may be used to practical issues such the cooling of bodies. Trigonometrically two-step hybrid techniques were presented by Ambrosio et al. [22] to solve second-order ODEs; these approaches might be modified for use in chemical kinetics simulations. Pushpam and Dhayabaran [23] employed an approach based on Walsh series for solving nonlinear HIRES problem In [24], Aslam et al. introduced Sumudu transform technique for solving HIRES problem under fractal fractional derivative. These approaches provide viable means of enhancing the precision and effectiveness of numerical solutions in chemical kinetics issues like HIRES, in conjunction with developments in numerical techniques.

In recent years, the application of wavelet analysis has emerged as a promising approach to unraveling the intricacies of HIRES problem. Wavelets [25, 26, 27, 28] permit for the exact modelling of a wide range of functions and operators. As a result, wavelets play an important role in several domains. The wavelet bases are still in its early stages, although it has attracted attention for solving several types of differential equations with the method of Taylor wavelets [29, 30], Legendre wavelets [31, 32], Gegenbauer wavelets [33], Bernstein wavelets

[34], Mamadu-Njoseh wavelets [35], Muntz wavelets [36, 37], Chebyshev wavelets [38, 39] and so on. Wavelets offer distinct advantages in analyzing the multi-scale and non-stationary nature of plant responses to varying light intensities. By decomposing complex signals generated by HIRES problem into different frequency components, wavelets enable researchers to identify key features and patterns associated with specific physiological responses, such as stem elongation inhibition, leaf expansion, chlorophyll accumulation, and floral induction. Furthermore, the adaptability of wavelets to capture both local and global information inherent in HIRES makes them particularly suited for elucidating the hierarchical and interconnected regulatory networks governing photomorphogenesis. In chemical kinetics, wavelet analysis has shown to be an invaluable technique for improving numerical solutions, especially when dealing with difficult issues like the HIRES problem.

To the best of our knowledge, no works deal with the application of wavelets ultraspherical wavelets (USWs) in solving nonlinear Hires problem of fractional order. Therefore, inspired by the above literatures, this study illustrates an application of USWs with suitable collocation grids for simulating HIRES problem under fractional Caputo derivative. Another motivation is that the Legendre wavelets and Chebyshev wavelets can be deduced as particular cases of the USWs. There are no substantial weaknesses appear in the suggested approach. However, this approach functions well in a limited domain and handling a large number of wavelet basis could lead to high computational cost. This study presents some following novelty to simulate the fractional HIRES problem.

- By employing the proposed scheme, considered fractional nonlinear model is reduced into a set of algebraic equations for less demanding calculations that can be simply solved by Newton iterative method.
- The USWs are simple basis functions from a computational point of view; therefore, these wavelets basis could be seen as an appropriate and convenient tool in this work for solving the fractional HIRES problem.

The structure of this work is provided as follows: Section 2 consists of a brief definition of the fractional operators, which will be employed in later sections, along with the proposed methodology. Section 3 presents the overview of Ultraspherical wavelets and function approximation. Section 4 introduces the novel wavelets collocation scheme applied to solve the fractional HIRES problem. Section 5 provides the error and convergence analysis for the model. In Section 6, the computational simulation of the underlying model under different fractional order is given. The conclusion of this study is outlined in Section 7.

## 2 Preliminaries

In this study, the following concepts of fractional operators are used.

### 2.1 Definition

If the function  $\Upsilon(\rho)$  is defined on  $(0,1]$ , then the fractional Caputo differentiation of  $\Upsilon(\rho)$  with order  $\lambda \in (0, 1]$  is given by [3]

$$D_{0,\rho}^\lambda \Upsilon(\rho) = \left\{ \frac{1}{\Gamma(1-\lambda)} \int_0^\rho \Upsilon'(\tau)(\rho-\tau)^{-\lambda} d\tau, \quad 0 < \lambda < 1, \right. \tag{2.1}$$

where  $\Gamma(\cdot)$  denotes the Gamma function. The Caputo fractional derivative is widely used in fractional calculus to describe systems with memory and hereditary properties.

### 2.2 Definition

The fractional integral of  $\Upsilon(\rho)$  under order  $\lambda \in (0, 1]$  is provided as [3]

$$I_{0,\rho}^\lambda \Upsilon(\rho) = \frac{1}{\Gamma(\lambda)} \int_0^\rho (\rho-\tau)^{\lambda-1} \Upsilon(\tau) d\tau, \quad 0 < \rho. \tag{2.2}$$

The connection between the operators in Eqs. (2.1) and (2.2) for  $\tau > 0$  is

$$(I_{0,\rho}^\lambda D_{0,\rho}^\lambda) \Upsilon(\rho) = \Upsilon(\rho) - \sum_{j=0}^{[\tau]-1} \frac{\rho^j}{\Gamma(j)} \Upsilon^{(j)}(0), \quad 0 < \rho. \tag{2.3}$$

### 3 Mathematical background of ultraspherical Wavelets and function approximation

The ultraspherical wavelets (USWs) derived from ultraspherical polynomials can be constructed to localize functions both in frequency and time domains. The USWs is denoted by  $\psi_{n,m}^\gamma(\rho)$  and defined on  $[0, 1]$  as [40, 41, 42]

$$\psi_{n,m}^\gamma(\rho) = \begin{cases} 2^{\frac{k+1}{2}} \mu_{m,\gamma} U_m^\gamma(2^{k+1}\rho - 2n + 1), & \frac{n-1}{2^k} \leq \rho \leq \frac{n}{2^k}, \\ 0, & \text{elsewhere} \end{cases} \tag{3.1}$$

where  $n = 1, 2, 3, \dots, 2^k$ ;  $m = 0, 1, 2, \dots, M - 1$ ;  $k$  is non-negative integer and

$$\mu_{m,\gamma} = 2^\gamma \Gamma(\gamma) \sqrt{\frac{m!(m+\gamma)}{2\pi \Gamma(m+2\gamma)}}. \tag{3.2}$$

Here,  $U_m^\gamma(\rho)$  is the ultraspherical polynomial defined on  $[-1, 1]$  having degree  $m$  and satisfies the following recurrence relations [40, 41]

$$\begin{aligned} U_0^\gamma(\rho) &= 1, \\ U_1^\gamma(\rho) &= 2\gamma\rho, \\ U_{n+1}^\gamma(\rho) &= \frac{2(n+\gamma)\rho U_n^\gamma(\rho) - (n-1+2\gamma)U_{n-1}^\gamma(\rho)}{n+1}, \quad n = 1, 2, \dots \end{aligned}$$

These ultraspherical polynomials are sequence of orthogonal polynomials under the weighted function  $w(\rho) = (1 - \rho^2)^{\gamma - \frac{1}{2}}$ .

Some of basis of USWs which are used in this study for  $k = 0, M = 3, \gamma = 1$  is given as

$$\begin{pmatrix} \psi_{10}(\rho) \\ \psi_{11}(\rho) \\ \psi_{12}(\rho) \end{pmatrix} = \begin{pmatrix} \frac{2}{\sqrt{\pi}} \\ \frac{4}{\sqrt{\pi}}(2\rho - 1) \\ \frac{2}{\sqrt{\pi}}(16\rho^2 - 16\rho + 3) \end{pmatrix}.$$

The set of USWs is orthogonal on  $[0, 1]$  under weighted function  $w_{n,k}(\rho) = w(2^{k+1}\rho - 2n + 1)$ .

Now, the approximation of unknown function is given by series of USWs. By using the concept of function approximation, any unknown function is easily calculated with considered wavelet basis.

Let  $\{\psi_{1,0}^\gamma(\rho), \dots, \psi_{1,M-1}^\gamma(\rho), \psi_{2,0}^\gamma(\rho), \dots, \psi_{2,M-1}^\gamma(\rho), \dots, \psi_{2^{k-1},0}^\gamma(\rho), \dots, \psi_{2^{k-1},(M-1)}^\gamma(\rho)\} \subset L^2[0, 1]$  is the set of USWs,

$S = Span\{\psi_{1,0}^\gamma(\rho), \dots, \psi_{1,M-1}^\gamma(\rho), \psi_{2,0}^\gamma(\rho), \dots, \psi_{2,M-1}^\gamma(\rho), \dots, \psi_{2^{k-1},0}^\gamma(\rho), \dots, \psi_{2^{k-1},(M-1)}^\gamma(\rho)\},$

&  $\Upsilon(\rho) \in L^2[0, 1]$  is an arbitrary element. Then  $\Upsilon(\rho)$  has a best approximation out of finite dimensional vector space  $S$  such as

$$\|\Upsilon(\rho) - \Upsilon_0(\rho)\| < \|\Upsilon(\rho) - h(\rho)\|; \Upsilon_0(\rho), h(\rho) \in S.$$

Any function  $\Upsilon(\rho) \in L^2[0, 1]$  can be formulated in a combination of USWs as

$$\Upsilon(\rho) \simeq \sum_{n=1}^{\infty} \sum_{m=0}^{\infty} e_{n,m} \psi_{n,m}^\gamma(\rho), \tag{3.3}$$

where the wavelets coefficients  $e_{n,m}$  corresponding to  $\psi_{n,m}^\gamma(\rho)$  are obtained by

$$\begin{aligned} e_{n,m} &= \langle \Upsilon(\rho), \psi_{n,m}^\gamma \rangle_{w_{n,k}(\rho)} \\ &= \int_0^1 \Upsilon(\rho) \psi_{n,m}^\gamma(\rho) w_{n,k}(\rho) d\rho. \end{aligned}$$

For approximation purposes, the truncated version of Eq. (3.3) is written as

$$\Upsilon(\rho) \simeq \sum_{n=1}^{2^{k-1}} \sum_{m=0}^{M-1} e_{n,m} \psi_{n,m}^\gamma(\rho). \tag{3.4}$$

In vector form, Eq. (3.4) can be written as

$$\Upsilon(\rho) \simeq E_{\hat{\mu} \times 1}^T \Psi_{\hat{\mu} \times 1}^\gamma(\rho), \tag{3.5}$$

where  $E$  and  $\Psi^\gamma(\rho)$  are  $\hat{\mu} \times 1$  vectors given by

$$\begin{aligned} E_{\hat{\mu} \times 1} &= [e_{1,0}, e_{1,1}, \dots, e_{1,M-1}, e_{2,0}, e_{2,1}, \dots, e_{2,M-1}, \dots, e_{2^{k-1},0}, e_{2^{k-1},1}, \dots, e_{2^{k-1},M-1}]^T \\ &= [e_1, e_2, \dots, e_{\hat{\mu}}]^T, \end{aligned} \tag{3.6}$$

$$\begin{aligned} \Psi_{\hat{\mu} \times 1}^\gamma(\rho) &= [\psi_{1,0}^\gamma(\rho), \dots, \psi_{1,M-1}^\gamma(\rho), \psi_{2,0}^\gamma(\rho), \dots, \psi_{2,M-1}^\gamma(\rho), \dots, \psi_{2^{k-1},0}^\gamma(\rho), \dots, \psi_{2^{k-1},(M-1)}^\gamma(\rho)]^T \\ &= [\psi_1^\gamma, \psi_2^\gamma, \dots, \psi_{\hat{\mu}}^\gamma]^T. \end{aligned} \tag{3.7}$$

During the computation steps, take  $2^{k-1}M = \hat{\mu}$  which shows the total USWs basis.

The following section introduces the USWs scheme for evaluating the fractional order system of the HIRES problem.

### 4 Numerical solution for Fractional HIRES Problem

The USWs approach is presented in the following steps to obtain the solutions of the model in Eq. (1.1) with Eq. (1.2) as:

First, estimate the unknown functions  $D_{0,\rho}^\lambda \Upsilon_j(\rho)$  of Eq. (1.1) in a series of truncated USWs using Eq. (3.5) as

$$\begin{aligned} D_{0,\rho}^\lambda \Upsilon_1(\rho) &\simeq E_1^T \Psi_{\hat{\mu} \times 1}^\gamma(\rho), \\ D_{0,\rho}^\lambda \Upsilon_2(\rho) &\simeq E_2^T \Psi_{\hat{\mu} \times 1}^\gamma(\rho), \\ D_{0,\rho}^\lambda \Upsilon_3(\rho) &\simeq E_3^T \Psi_{\hat{\mu} \times 1}^\gamma(\rho), \\ D_{0,\rho}^\lambda \Upsilon_4(\rho) &\simeq E_4^T \Psi_{\hat{\mu} \times 1}^\gamma(\rho), \\ D_{0,\rho}^\lambda \Upsilon_5(\rho) &\simeq E_5^T \Psi_{\hat{\mu} \times 1}^\gamma(\rho), \\ D_{0,\rho}^\lambda \Upsilon_6(\rho) &\simeq E_6^T \Psi_{\hat{\mu} \times 1}^\gamma(\rho), \\ D_{0,\rho}^\lambda \Upsilon_7(\rho) &\simeq E_7^T \Psi_{\hat{\mu} \times 1}^\gamma(\rho), \\ D_{0,\rho}^\lambda \Upsilon_8(\rho) &\simeq E_8^T \Psi_{\hat{\mu} \times 1}^\gamma(\rho), \end{aligned} \tag{4.1}$$

where  $\Psi_{\hat{\mu} \times 1}^\gamma(\rho)$  is provided in Eqs. (3.7) and (3.1) and wavelet coefficients vector  $E_j$  for  $j = 1, 2, \dots, 8$  is taken as Eq. (3.6).

By utilizing Eq. (2.2) on Eq. (4.1), and use Eqs. (2.3) and (1.2), we obtain

$$\begin{aligned}
 (I_{0,\rho}^\lambda D_{0,\rho}^\lambda) \Upsilon_1(\rho) &\simeq I_{0,\rho}^\lambda \left( E_1^T \Psi_{\hat{\mu} \times 1}^\gamma(\rho) \right), \\
 (I_{0,\rho}^\lambda D_{0,\rho}^\lambda) \Upsilon_2(\rho) &\simeq I_{0,\rho}^\lambda \left( E_2^T \Psi_{\hat{\mu} \times 1}^\gamma(\rho) \right), \\
 (I_{0,\rho}^\lambda D_{0,\rho}^\lambda) \Upsilon_3(\rho) &\simeq I_{0,\rho}^\lambda \left( E_3^T \Psi_{\hat{\mu} \times 1}^\gamma(\rho) \right), \\
 (I_{0,\rho}^\lambda D_{0,\rho}^\lambda) \Upsilon_4(\rho) &\simeq I_{0,\rho}^\lambda \left( E_4^T \Psi_{\hat{\mu} \times 1}^\gamma(\rho) \right), \\
 (I_{0,\rho}^\lambda D_{0,\rho}^\lambda) \Upsilon_5(\rho) &\simeq I_{0,\rho}^\lambda \left( E_5^T \Psi_{\hat{\mu} \times 1}^\gamma(\rho) \right), \\
 (I_{0,\rho}^\lambda D_{0,\rho}^\lambda) \Upsilon_6(\rho) &\simeq I_{0,\rho}^\lambda \left( E_6^T \Psi_{\hat{\mu} \times 1}^\gamma(\rho) \right), \\
 (I_{0,\rho}^\lambda D_{0,\rho}^\lambda) \Upsilon_7(\rho) &\simeq I_{0,\rho}^\lambda \left( E_7^T \Psi_{\hat{\mu} \times 1}^\gamma(\rho) \right), \\
 (I_{0,\rho}^\lambda D_{0,\rho}^\lambda) \Upsilon_8(\rho) &\simeq I_{0,\rho}^\lambda \left( E_8^T \Psi_{\hat{\mu} \times 1}^\gamma(\rho) \right).
 \end{aligned}$$

This implies the following form

$$\begin{aligned}
 \Upsilon_1(\rho) &\simeq \Upsilon_1(0) + E_1^T \left( I_{0,\rho}^\lambda \Psi_{\hat{\mu} \times 1}^\gamma(\rho) \right), \\
 \Upsilon_2(\rho) &\simeq \Upsilon_2(0) + E_2^T \left( I_{0,\rho}^\lambda \Psi_{\hat{\mu} \times 1}^\gamma(\rho) \right), \\
 \Upsilon_3(\rho) &\simeq \Upsilon_3(0) + E_3^T \left( I_{0,\rho}^\lambda \Psi_{\hat{\mu} \times 1}^\gamma(\rho) \right), \\
 \Upsilon_4(\rho) &\simeq \Upsilon_4(0) + E_4^T \left( I_{0,\rho}^\lambda \Psi_{\hat{\mu} \times 1}^\gamma(\rho) \right), \\
 \Upsilon_5(\rho) &\simeq \Upsilon_5(0) + E_5^T \left( I_{0,\rho}^\lambda \Psi_{\hat{\mu} \times 1}^\gamma(\rho) \right), \\
 \Upsilon_6(\rho) &\simeq \Upsilon_6(0) + E_6^T \left( I_{0,\rho}^\lambda \Psi_{\hat{\mu} \times 1}^\gamma(\rho) \right), \\
 \Upsilon_7(\rho) &\simeq \Upsilon_7(0) + E_7^T \left( I_{0,\rho}^\lambda \Psi_{\hat{\mu} \times 1}^\gamma(\rho) \right), \\
 \Upsilon_8(\rho) &\simeq \Upsilon_8(0) + E_8^T \left( I_{0,\rho}^\lambda \Psi_{\hat{\mu} \times 1}^\gamma(\rho) \right),
 \end{aligned} \tag{4.2}$$

where  $I_{0,\rho}^\lambda \Psi_{\hat{\mu} \times 1}^\gamma(\rho)$  is computed by direct integrating the known wavelet function  $\Psi_{\hat{\mu} \times 1}^\gamma(\rho)$  for different  $\hat{\mu}$ .

Substituting Eqs. (4.1) and (4.2) in the given system of Eq. (1.1), we get

$$\begin{aligned}
 E_1^T \Psi_{\hat{\mu} \times 1}^\gamma(\rho) &= -\beta_1 \left[ \Upsilon_1(0) + E_1^T \left( I_{0,\rho}^\lambda \Psi_{\hat{\mu} \times 1}^\gamma(\rho) \right) \right] + \beta_2 \left[ \Upsilon_2(0) + E_2^T \left( I_{0,\rho}^\lambda \Psi_{\hat{\mu} \times 1}^\gamma(\rho) \right) \right] \\
 &\quad + \beta_3 \left[ \Upsilon_3(0) + E_3^T \left( I_{0,\rho}^\lambda \Psi_{\hat{\mu} \times 1}^\gamma(\rho) \right) \right] + \beta_4, \\
 E_2^T \Psi_{\hat{\mu} \times 1}^\gamma(\rho) &= \beta_1 \left[ \Upsilon_1(0) + E_1^T \left( I_{0,\rho}^\lambda \Psi_{\hat{\mu} \times 1}^\gamma(\rho) \right) \right] - \beta_5 \left[ \Upsilon_2(0) + E_2^T \left( I_{0,\rho}^\lambda \Psi_{\hat{\mu} \times 1}^\gamma(\rho) \right) \right], \\
 E_3^T \Psi_{\hat{\mu} \times 1}^\gamma(\rho) &= -\beta_6 \left[ \Upsilon_3(0) + E_3^T \left( I_{0,\rho}^\lambda \Psi_{\hat{\mu} \times 1}^\gamma(\rho) \right) \right] + \beta_2 \left[ \Upsilon_4(0) + E_4^T \left( I_{0,\rho}^\lambda \Psi_{\hat{\mu} \times 1}^\gamma(\rho) \right) \right] \\
 &\quad + \beta_7 \left[ \Upsilon_5(0) + E_5^T \left( I_{0,\rho}^\lambda \Psi_{\hat{\mu} \times 1}^\gamma(\rho) \right) \right], \\
 E_4^T \Psi_{\hat{\mu} \times 1}^\gamma(\rho) &= \beta_3 \left[ \Upsilon_2(0) + E_2^T \left( I_{0,\rho}^\lambda \Psi_{\hat{\mu} \times 1}^\gamma(\rho) \right) \right] + \beta_8 \left[ \Upsilon_3(0) + E_3^T \left( I_{0,\rho}^\lambda \Psi_{\hat{\mu} \times 1}^\gamma(\rho) \right) \right] \\
 &\quad - \beta_9 \left[ \Upsilon_4(0) + E_4^T \left( I_{0,\rho}^\lambda \Psi_{\hat{\mu} \times 1}^\gamma(\rho) \right) \right], \\
 E_5^T \Psi_{\hat{\mu} \times 1}^\gamma(\rho) &= -\beta_{10} \left[ \Upsilon_5(0) + E_5^T \left( I_{0,\rho}^\lambda \Psi_{\hat{\mu} \times 1}^\gamma(\rho) \right) \right] + \beta_2 \left[ \Upsilon_6(0) + E_6^T \left( I_{0,\rho}^\lambda \Psi_{\hat{\mu} \times 1}^\gamma(\rho) \right) \right] \\
 &\quad + \beta_2 \left[ \Upsilon_7(0) + E_7^T \left( I_{0,\rho}^\lambda \Psi_{\hat{\mu} \times 1}^\gamma(\rho) \right) \right], \tag{4.3} \\
 E_6^T \Psi_{\hat{\mu} \times 1}^\gamma(\rho) &= -\beta_{11} \left[ \Upsilon_6(0) + E_6^T \left( I_{0,\rho}^\lambda \Psi_{\hat{\mu} \times 1}^\gamma(\rho) \right) \right] \left[ \Upsilon_8(0.0057) + E_8^T \left( I_{0,\rho}^\lambda \Psi_{\hat{\mu} \times 1}^\gamma(\rho) \right) \right] \\
 &\quad + \beta_{12} \left[ \Upsilon_4(0) + E_4^T \left( I_{0,\rho}^\lambda \Psi_{\hat{\mu} \times 1}^\gamma(\rho) \right) \right] + \beta_8 \left[ \Upsilon_5(0) + E_5^T \left( I_{0,\rho}^\lambda \Psi_{\hat{\mu} \times 1}^\gamma(\rho) \right) \right] \\
 &\quad - \beta_2 \left[ \Upsilon_6(0) + E_6^T \left( I_{0,\rho}^\lambda \Psi_{\hat{\mu} \times 1}^\gamma(\rho) \right) \right] + \beta_{12} \left[ \Upsilon_7(0) + E_7^T \left( I_{0,\rho}^\lambda \Psi_{\hat{\mu} \times 1}^\gamma(\rho) \right) \right], \\
 E_7^T \Psi_{\hat{\mu} \times 1}^\gamma(\rho) &= \beta_{11} \left[ \Upsilon_6(0) + E_6^T \left( I_{0,\rho}^\lambda \Psi_{\hat{\mu} \times 1}^\gamma(\rho) \right) \right] \left[ \Upsilon_8(0.0057) + E_8^T \left( I_{0,\rho}^\lambda \Psi_{\hat{\mu} \times 1}^\gamma(\rho) \right) \right] \\
 &\quad - \beta_{13} \left[ \Upsilon_7(0) + E_7^T \left( I_{0,\rho}^\lambda \Psi_{\hat{\mu} \times 1}^\gamma(\rho) \right) \right], \\
 E_8^T \Psi_{\hat{\mu} \times 1}^\gamma(\rho) &= -\beta_{11} \left[ \Upsilon_6(0) + E_6^T \left( I_{0,\rho}^\lambda \Psi_{\hat{\mu} \times 1}^\gamma(\rho) \right) \right] \left[ \Upsilon_8(0.0057) + E_8^T \left( I_{0,\rho}^\lambda \Psi_{\hat{\mu} \times 1}^\gamma(\rho) \right) \right] \\
 &\quad + \beta_{13} \left[ \Upsilon_7(0) + E_7^T \left( I_{0,\rho}^\lambda \Psi_{\hat{\mu} \times 1}^\gamma(\rho) \right) \right],
 \end{aligned}$$

By collocating Eq. (4.3) at suitable collocation grids  $\rho_i$ , a set of  $\hat{\mu}$  non-linear algebraic

equations is obtained as

$$\begin{aligned}
 E_1^T \Psi_{\hat{\mu} \times 1}^\gamma(\rho_i) &= -\beta_1 \left[ \Upsilon_1(0) + E_1^T \left( I_{0,\rho}^\lambda \Psi_{\hat{\mu} \times 1}^\gamma(\rho_i) \right) \right] + \beta_2 \left[ \Upsilon_2(0) + E_2^T \left( I_{0,\rho}^\lambda \Psi_{\hat{\mu} \times 1}^\gamma(\rho_i) \right) \right] \\
 &\quad + \beta_3 \left[ \Upsilon_3(0) + E_3^T \left( I_{0,\rho}^\lambda \Psi_{\hat{\mu} \times 1}^\gamma(\rho_i) \right) \right] + \beta_4, \\
 E_2^T \Psi_{\hat{\mu} \times 1}^\gamma(\rho_i) &= \beta_1 \left[ \Upsilon_1(0) + E_1^T \left( I_{0,\rho}^\lambda \Psi_{\hat{\mu} \times 1}^\gamma(\rho_i) \right) \right] - \beta_5 \left[ \Upsilon_2(0) + E_2^T \left( I_{0,\rho}^\lambda \Psi_{\hat{\mu} \times 1}^\gamma(\rho_i) \right) \right], \\
 E_3^T \Psi_{\hat{\mu} \times 1}^\gamma(\rho_i) &= -\beta_6 \left[ \Upsilon_3(0) + E_3^T \left( I_{0,\rho}^\lambda \Psi_{\hat{\mu} \times 1}^\gamma(\rho_i) \right) \right] + \beta_2 \left[ \Upsilon_4(0) + E_4^T \left( I_{0,\rho}^\lambda \Psi_{\hat{\mu} \times 1}^\gamma(\rho_i) \right) \right] \\
 &\quad + \beta_7 \left[ \Upsilon_5(0) + E_5^T \left( I_{0,\rho}^\lambda \Psi_{\hat{\mu} \times 1}^\gamma(\rho_i) \right) \right], \\
 E_4^T \Psi_{\hat{\mu} \times 1}^\gamma(\rho_i) &= \beta_3 \left[ \Upsilon_2(0) + E_2^T \left( I_{0,\rho}^\lambda \Psi_{\hat{\mu} \times 1}^\gamma(\rho_i) \right) \right] + \beta_8 \left[ \Upsilon_3(0) + E_3^T \left( I_{0,\rho}^\lambda \Psi_{\hat{\mu} \times 1}^\gamma(\rho_i) \right) \right] \\
 &\quad - \beta_9 \left[ \Upsilon_4(0) + E_4^T \left( I_{0,\rho}^\lambda \Psi_{\hat{\mu} \times 1}^\gamma(\rho_i) \right) \right], \\
 E_5^T \Psi_{\hat{\mu} \times 1}^\gamma(\rho_i) &= -\beta_{10} \left[ \Upsilon_5(0) + E_5^T \left( I_{0,\rho}^\lambda \Psi_{\hat{\mu} \times 1}^\gamma(\rho_i) \right) \right] + \beta_2 \left[ \Upsilon_6(0) + E_6^T \left( I_{0,\rho}^\lambda \Psi_{\hat{\mu} \times 1}^\gamma(\rho_i) \right) \right] \\
 &\quad + \beta_2 \left[ \Upsilon_7(0) + E_7^T \left( I_{0,\rho}^\lambda \Psi_{\hat{\mu} \times 1}^\gamma(\rho_i) \right) \right], \tag{4.4} \\
 E_6^T \Psi_{\hat{\mu} \times 1}^\gamma(\rho_i) &= -\beta_{11} \left[ \Upsilon_6(0) + E_6^T \left( I_{0,\rho}^\lambda \Psi_{\hat{\mu} \times 1}^\gamma(\rho_i) \right) \right] \left[ \Upsilon_8(0.0057) + E_8^T \left( I_{0,\rho}^\lambda \Psi_{\hat{\mu} \times 1}^\gamma(\rho_i) \right) \right] \\
 &\quad + \beta_{12} \left[ \Upsilon_4(0) + E_4^T \left( I_{0,\rho}^\lambda \Psi_{\hat{\mu} \times 1}^\gamma(\rho_i) \right) \right] + \beta_8 \left[ \Upsilon_5(0) + E_5^T \left( I_{0,\rho}^\lambda \Psi_{\hat{\mu} \times 1}^\gamma(\rho_i) \right) \right] \\
 &\quad - \beta_2 \left[ \Upsilon_6(0) + E_6^T \left( I_{0,\rho}^\lambda \Psi_{\hat{\mu} \times 1}^\gamma(\rho_i) \right) \right] + \beta_{12} \left[ \Upsilon_7(0) + E_7^T \left( I_{0,\rho}^\lambda \Psi_{\hat{\mu} \times 1}^\gamma(\rho_i) \right) \right], \\
 E_7^T \Psi_{\hat{\mu} \times 1}^\gamma(\rho_i) &= \beta_{11} \left[ \Upsilon_6(0) + E_6^T \left( I_{0,\rho}^\lambda \Psi_{\hat{\mu} \times 1}^\gamma(\rho_i) \right) \right] \left[ \Upsilon_8(0.0057) + E_8^T \left( I_{0,\rho}^\lambda \Psi_{\hat{\mu} \times 1}^\gamma(\rho_i) \right) \right] \\
 &\quad - \beta_{13} \left[ \Upsilon_7(0) + E_7^T \left( I_{0,\rho}^\lambda \Psi_{\hat{\mu} \times 1}^\gamma(\rho_i) \right) \right], \\
 E_8^T \Psi_{\hat{\mu} \times 1}^\gamma(\rho_i) &= -\beta_{11} \left[ \Upsilon_6(0) + E_6^T \left( I_{0,\rho}^\lambda \Psi_{\hat{\mu} \times 1}^\gamma(\rho_i) \right) \right] \left[ \Upsilon_8(0.0057) + E_8^T \left( I_{0,\rho}^\lambda \Psi_{\hat{\mu} \times 1}^\gamma(\rho_i) \right) \right] \\
 &\quad + \beta_{13} \left[ \Upsilon_7(0) + E_7^T \left( I_{0,\rho}^\lambda \Psi_{\hat{\mu} \times 1}^\gamma(\rho_i) \right) \right],
 \end{aligned}$$

where appropriate collocation grids  $\rho_i$  is provided by

$$\rho_i = \left( \frac{2i - 1}{2\hat{\mu}} \right); \quad i = 1, 2, \dots, \hat{\mu}. \tag{4.5}$$

Now, solve the set of algebraic equations formed in Eq. (4.4) by well-suitable iterative method, we can readily determine the unknown wavelet coefficient vectors  $E_1^T, E_2^T, E_3^T, E_4^T, E_5^T, E_6^T, E_7^T$  &  $E_8^T$ .

Using the value of obtained coefficient vector in Eq. (4.2), we determine the wavelets approximate solution of  $\Upsilon_1(\rho), \Upsilon_2(\rho), \Upsilon_3(\rho), \Upsilon_4(\rho), \Upsilon_5(\rho), \Upsilon_6(\rho), \Upsilon_7(\rho)$  &  $\Upsilon_8(\rho)$ . Procedure completed.

**Remark:** The collocation points given in Eq. (4.5) are usually implemented in most of the numerical methods due to their better performance from the computational point of view for obtaining the approximate solution of the models. Also, these collocation points correspond to equally spaced grids, which are straightforward to implement and distribute over the interval. This simplicity can make the formulation and computation easier. That is the reason for selecting these collocation points. Selecting the zeros of ultraspherical polynomials or any other orthogonal polynomials can improve the accuracy of numerical algorithms in approximation methods and numerical integration. The zeros of orthogonal polynomials yield significant results with lower errors as compared to using arbitrary spaced points.

The algorithm for the described scheme is given in Figure 1.

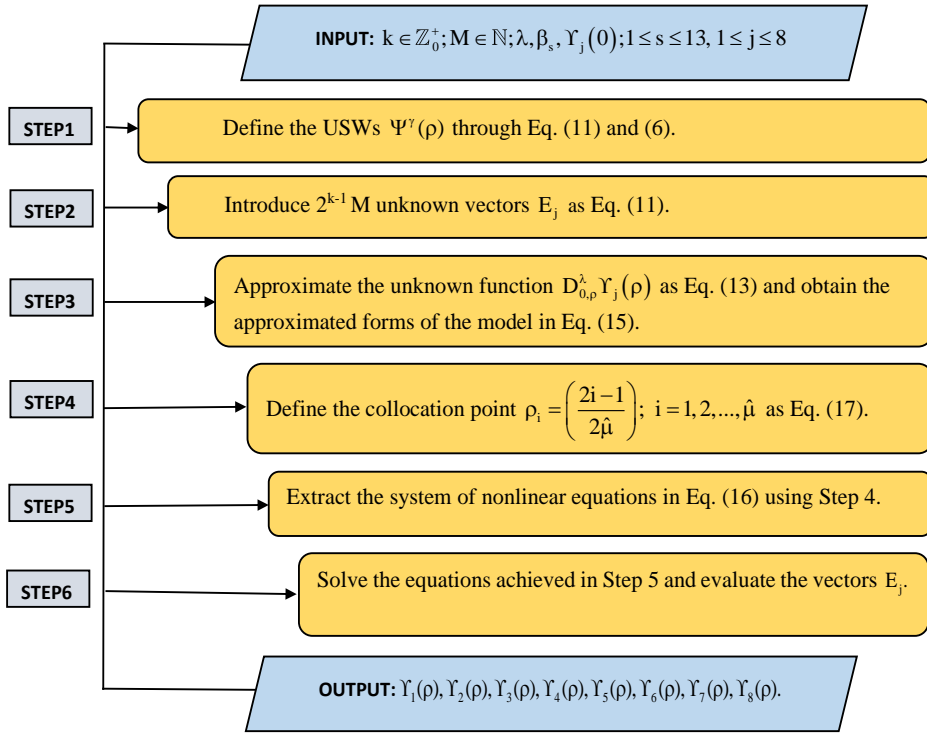


Figure 1: Algorithm for the described scheme.

### 5 Error and Convergence analysis

The accuracy of the implemented approach is evaluated by analyzing several error functions: max and min residual error (RE), and  $L_2$  residual error.

- Since the exact solution is not available for this model, so the reliability of the suggested approach is examined by the residual error function  $E_{REF}(\rho)$  as follows

$$E_{REF}(\rho) = |D_{0,\rho}^\lambda Y_j(\rho) - f(Y_j(\rho), \rho)|.$$

- The maximum RE is estimated as

$$Max\ RE = \max_{0 \leq \rho \leq 1} (E_{REF}(\rho)).$$

- The minimum RE is computed by

$$Min\ RE = \min_{0 \leq \rho \leq 1} (E_{REF}(\rho)).$$

- The  $L_2$  residual error is obtained as

$$L_2 = \sqrt[2]{\int_0^1 (E_{REF}(\rho))^2 d\rho}.$$

By using these error formulas, we can examine the accuracy of the suggested method for fractional nonlinear HIRES problem.

The fundamental findings corresponding to the approximation of Ultraspherical polynomials serve as the foundation for exploring the convergence of USWs approximations.

**Theorem 1:** For any function  $Y(\rho) \in L^2[0, 1]$ , let the USWs expansion

$$\sum_{n=0}^{2^{k-1}-1} \sum_{m=0}^{M-1} e_{n,m} \psi_{n,m}^\gamma(\rho) = \sum_{j=0}^{\hat{m}} e_j \psi_j^\gamma(\rho) = E^T \Psi^\gamma(\rho)$$

of the function  $\Upsilon(\rho)$ , then the error estimate is obtained as

$$\left\| \Upsilon(\rho) - \sum_{j=0}^{\hat{m}} e_j \psi_j^\gamma(\rho) \right\|_2 \leq \frac{\Omega(1 + \gamma)^2(M + \gamma)}{(M - 3)^{7/2} 2^{4k}},$$

Also,

$$\lim_{\hat{m} \rightarrow \infty} \left\| \Upsilon(\rho) - \sum_{j=0}^{\hat{m}} e_j \psi_j^\gamma(\rho) \right\|_2 = 0,$$

where  $\hat{m} = 2^{k-1}M$  and  $\Omega = \max_{\rho \in [0,1]} |\Upsilon^{n+1}(\rho)|$ .

**Proof:** For proof, see [43].

### 6 Numerical Results

In this section, we present the results from the numerical experiments conducted using the approach described in Section 4. This method is employed for fractional HIRES problems to demonstrate the efficiency of the proposed method. The considered model is simulated by taking the following values of parameters involved in Eq. (1.1) according to [18] which is given in Table 1.

Table 1: Values of parameters involved in the model.

$\beta_1$	$\beta_2$	$\beta_3$	$\beta_4$	$\beta_5$	$\beta_6$	$\beta_7$
1.7	0.43	8.32	0.0007	8.75	10.03	0.035
$\beta_8$	$\beta_9$	$\beta_{10}$	$\beta_{11}$	$\beta_{12}$	$\beta_{13}$	
1.71	1.12	1.745	280	0.69	1.81	

The initial values associated with Eq. (1.1) is given by

$$(\Upsilon_1(0), \Upsilon_2(0), \Upsilon_3(0), \Upsilon_4(0), \Upsilon_5(0), \Upsilon_6(0), \Upsilon_7(0), \Upsilon_8(0)) = (1, 0, 0, 0, 0, 0, 0, 0.0057).$$

We solve the considered model for  $\hat{\mu} = 2, 3$  by the mentioned approach. Since the analytical solution of this model is not available in any order, therefore we calculate the residual error for the solution of the model. The estimated residual errors in the solutions  $\Upsilon_j(\rho)$  of the model for different fractional order  $\lambda$  are listed in Tables 2-9 with max RE, min RE and  $L_2$  residual error. From Tables 2-9, it is observed that the error decreases as the wavelet basis or collocation points increase. The graphical interpretation of approximated solutions and its corresponding residual errors is depicted in Figures 2-9 for different fractional order  $\lambda$  and  $\hat{\mu} = 3$ .

The impact of fractional order can be easily noticeable when simulating eight compartments having a concentration of chemical reaction described by stiff differential equations. As the fractional order decreases, the concentration  $\Upsilon_j(\rho)$  for  $j = 1, 2, \dots, 6$  and  $\Upsilon_8(\rho)$  of the chemical species begin to decrease and the concentration  $\Upsilon_7(\rho)$  of the chemical species begins to increase as the fractional order decreases. It is also crucial for solving nonlinear problems, which are frequently encountered by researchers in kinetics chemistry.

Table 2: Estimated errors for the model at  $\hat{\mu} = 2, \lambda = 1$ .

$\rho$	$\Upsilon_1(\rho)$	$\Upsilon_2(\rho)$	$\Upsilon_3(\rho)$	$\Upsilon_4(\rho)$	$\Upsilon_5(\rho)$	$\Upsilon_6(\rho)$	$\Upsilon_7(\rho)$	$\Upsilon_8(\rho)$
0.2	$3.2 \times 10^{-2}$	$1.7 \times 10^{-0}$	$5.2 \times 10^{-5}$	$1.4 \times 10^{-2}$	$1.1 \times 10^{-3}$	$1.2 \times 10^{-2}$	$5.4 \times 10^{-3}$	$5.4 \times 10^{-3}$
0.4	$6.2 \times 10^{-2}$	$1.6 \times 10^{-0}$	$9.9 \times 10^{-5}$	$2.7 \times 10^{-2}$	$2.2 \times 10^{-3}$	$3.8 \times 10^{-2}$	$2.4 \times 10^{-2}$	$2.4 \times 10^{-2}$
0.6	$6.2 \times 10^{-2}$	$1.6 \times 10^{-0}$	$9.9 \times 10^{-5}$	$2.7 \times 10^{-2}$	$2.2 \times 10^{-3}$	$5.7 \times 10^{-2}$	$4.3 \times 10^{-2}$	$4.3 \times 10^{-2}$
0.8	$3.2 \times 10^{-2}$	$1.7 \times 10^{-0}$	$5.2 \times 10^{-5}$	$1.4 \times 10^{-2}$	$1.1 \times 10^{-3}$	$4.3 \times 10^{-2}$	$3.6 \times 10^{-2}$	$3.6 \times 10^{-2}$
1.0	$2.2 \times 10^{-1}$	$1.8 \times 10^{-0}$	$3.5 \times 10^{-4}$	$9.9 \times 10^{-2}$	$7.9 \times 10^{-3}$	$4.0 \times 10^{-1}$	$3.5 \times 10^{-1}$	$3.5 \times 10^{-1}$
Max RE	$2.2 \times 10^{-1}$	$1.8 \times 10^{-0}$	$3.5 \times 10^{-4}$	$9.9 \times 10^{-2}$	$7.9 \times 10^{-3}$	$4.0 \times 10^{-1}$	$3.5 \times 10^{-1}$	$3.5 \times 10^{-1}$
Min RE	$4.1 \times 10^{-11}$	$1.6 \times 10^{-0}$	$6.2 \times 10^{-14}$	$1.8 \times 10^{-11}$	$1.4 \times 10^{-12}$	$1.1 \times 10^{-12}$	$2.1 \times 10^{-10}$	$2.1 \times 10^{-10}$
$L_2$ error	$9.2 \times 10^{-2}$	$1.7 \times 10^{-0}$	$1.4 \times 10^{-4}$	$4.1 \times 10^{-2}$	$3.2 \times 10^{-3}$	$1.0 \times 10^{-1}$	$8.8 \times 10^{-2}$	$8.8 \times 10^{-2}$

Table 3: Estimated errors for the model at  $\hat{\mu} = 3, \lambda = 1$ .

$\rho$	$\Upsilon_1(\rho)$	$\Upsilon_2(\rho)$	$\Upsilon_3(\rho)$	$\Upsilon_4(\rho)$	$\Upsilon_5(\rho)$	$\Upsilon_6(\rho)$	$\Upsilon_7(\rho)$	$\Upsilon_8(\rho)$
0.2	$4.8 \times 10^{-3}$	$1.6 \times 10^{-0}$	$4.2 \times 10^{-4}$	$5.8 \times 10^{-3}$	$3.7 \times 10^{-5}$	$2.2 \times 10^{-2}$	$1.9 \times 10^{-2}$	$1.9 \times 10^{-2}$
0.4	$7.7 \times 10^{-3}$	$1.6 \times 10^{-0}$	$6.7 \times 10^{-4}$	$9.3 \times 10^{-3}$	$6.0 \times 10^{-5}$	$6.8 \times 10^{-2}$	$6.4 \times 10^{-2}$	$6.4 \times 10^{-2}$
0.6	$7.7 \times 10^{-3}$	$1.7 \times 10^{-0}$	$6.7 \times 10^{-4}$	$9.3 \times 10^{-3}$	$6.0 \times 10^{-5}$	$1.0 \times 10^{-1}$	$9.5 \times 10^{-2}$	$9.5 \times 10^{-2}$
0.8	$4.8 \times 10^{-3}$	$1.7 \times 10^{-0}$	$4.2 \times 10^{-4}$	$5.8 \times 10^{-3}$	$3.7 \times 10^{-5}$	$7.1 \times 10^{-2}$	$6.8 \times 10^{-2}$	$6.8 \times 10^{-2}$
1.0	$5.2 \times 10^{-2}$	$1.5 \times 10^{-0}$	$4.6 \times 10^{-3}$	$6.4 \times 10^{-2}$	$4.1 \times 10^{-4}$	$6.5 \times 10^{-1}$	$6.2 \times 10^{-1}$	$6.2 \times 10^{-1}$
Max RE	$5.2 \times 10^{-2}$	$1.8 \times 10^{-0}$	$4.6 \times 10^{-3}$	$6.4 \times 10^{-2}$	$4.1 \times 10^{-4}$	$6.5 \times 10^{-1}$	$6.2 \times 10^{-1}$	$6.2 \times 10^{-1}$
Min RE	$0.0 \times 10^{-0}$	$1.5 \times 10^{-0}$	$6.9 \times 10^{-18}$	$1.1 \times 10^{-16}$	$5.2 \times 10^{-18}$	$4.2 \times 10^{-12}$	$7.5 \times 10^{-12}$	$7.5 \times 10^{-12}$
$L_2$ error	$1.6 \times 10^{-2}$	$1.7 \times 10^{-0}$	$1.4 \times 10^{-3}$	$2.0 \times 10^{-2}$	$1.3 \times 10^{-4}$	$1.6 \times 10^{-1}$	$1.5 \times 10^{-1}$	$1.5 \times 10^{-1}$

Table 4: Estimated errors for the model at  $\hat{\mu} = 2, \lambda = 0.9$ .

$\rho$	$\Upsilon_1(\rho)$	$\Upsilon_2(\rho)$	$\Upsilon_3(\rho)$	$\Upsilon_4(\rho)$	$\Upsilon_5(\rho)$	$\Upsilon_6(\rho)$	$\Upsilon_7(\rho)$	$\Upsilon_8(\rho)$
0.2	$3.8 \times 10^{-2}$	$1.7 \times 10^{-0}$	$3.7 \times 10^{-4}$	$2.8 \times 10^{-1}$	$1.1 \times 10^{-3}$	$1.4 \times 10^{-2}$	$8.7 \times 10^{-3}$	$7.5 \times 10^{-3}$
0.4	$6.9 \times 10^{-2}$	$1.6 \times 10^{-0}$	$6.4 \times 10^{-4}$	$4.7 \times 10^{-1}$	$2.1 \times 10^{-3}$	$4.8 \times 10^{-2}$	$3.7 \times 10^{-2}$	$3.9 \times 10^{-2}$
0.6	$6.6 \times 10^{-2}$	$1.6 \times 10^{-0}$	$6.0 \times 10^{-4}$	$6.1 \times 10^{-1}$	$2.1 \times 10^{-3}$	$7.5 \times 10^{-2}$	$6.3 \times 10^{-2}$	$6.7 \times 10^{-2}$
0.8	$3.4 \times 10^{-2}$	$1.7 \times 10^{-0}$	$3.0 \times 10^{-4}$	$6.9 \times 10^{-1}$	$1.1 \times 10^{-3}$	$5.6 \times 10^{-2}$	$5.0 \times 10^{-2}$	$4.7 \times 10^{-2}$
1.0	$2.2 \times 10^{-1}$	$1.8 \times 10^{-0}$	$1.9 \times 10^{-3}$	$7.2 \times 10^{-1}$	$7.5 \times 10^{-3}$	$5.2 \times 10^{-1}$	$4.8 \times 10^{-1}$	$4.8 \times 10^{-1}$
Max RE	$3.1 \times 10^{-1}$	$1.8 \times 10^{-0}$	$3.3 \times 10^{-3}$	$7.2 \times 10^{-1}$	$8.2 \times 10^{-3}$	$5.2 \times 10^{-1}$	$4.8 \times 10^{-1}$	$4.8 \times 10^{-1}$
Min RE	$3.9 \times 10^{-11}$	$1.6 \times 10^{-0}$	$3.3 \times 10^{-13}$	$1.3 \times 10^{-12}$	$1.3 \times 10^{-12}$	$6.8 \times 10^{-12}$	$1.6 \times 10^{-11}$	$1.6 \times 10^{-11}$
$L_2$ error	$1.0 \times 10^{-1}$	$1.7 \times 10^{-0}$	$1.0 \times 10^{-3}$	$5.3 \times 10^{-1}$	$3.2 \times 10^{-3}$	$1.3 \times 10^{-1}$	$1.2 \times 10^{-1}$	$1.2 \times 10^{-1}$

Table 5: Estimated errors for the model at  $\hat{\mu} = 3, \lambda = 0.9$ .

$\rho$	$\Upsilon_1(\rho)$	$\Upsilon_2(\rho)$	$\Upsilon_3(\rho)$	$\Upsilon_4(\rho)$	$\Upsilon_5(\rho)$	$\Upsilon_6(\rho)$	$\Upsilon_7(\rho)$	$\Upsilon_8(\rho)$
0.2	$8.5 \times 10^{-3}$	$1.6 \times 10^{-0}$	$2.7 \times 10^{-4}$	$1.4 \times 10^{-3}$	$1.1 \times 10^{-4}$	$1.6 \times 10^{-2}$	$1.3 \times 10^{-2}$	$1.3 \times 10^{-2}$
0.4	$1.2 \times 10^{-2}$	$1.6 \times 10^{-0}$	$4.4 \times 10^{-4}$	$2.7 \times 10^{-3}$	$1.7 \times 10^{-4}$	$4.9 \times 10^{-2}$	$4.5 \times 10^{-2}$	$4.5 \times 10^{-2}$
0.6	$1.1 \times 10^{-2}$	$1.7 \times 10^{-0}$	$4.4 \times 10^{-4}$	$3.0 \times 10^{-3}$	$1.6 \times 10^{-4}$	$7.6 \times 10^{-2}$	$7.2 \times 10^{-2}$	$7.2 \times 10^{-2}$
0.8	$6.8 \times 10^{-3}$	$1.7 \times 10^{-0}$	$2.7 \times 10^{-4}$	$1.9 \times 10^{-3}$	$9.8 \times 10^{-5}$	$6.4 \times 10^{-2}$	$6.1 \times 10^{-2}$	$6.1 \times 10^{-2}$
1.0	$7.2 \times 10^{-2}$	$1.5 \times 10^{-0}$	$2.9 \times 10^{-3}$	$2.2 \times 10^{-2}$	$1.0 \times 10^{-3}$	$8.4 \times 10^{-1}$	$8.1 \times 10^{-1}$	$8.1 \times 10^{-1}$
Max RE	$1.3 \times 10^{-1}$	$1.8 \times 10^{-0}$	$2.8 \times 10^{-3}$	$2.2 \times 10^{-2}$	$1.5 \times 10^{-3}$	$8.4 \times 10^{-1}$	$8.1 \times 10^{-1}$	$8.1 \times 10^{-1}$
Min RE	$1.4 \times 10^{-12}$	$1.5 \times 10^{-0}$	$4.8 \times 10^{-15}$	$4.0 \times 10^{-12}$	$1.5 \times 10^{-14}$	$4.4 \times 10^{-12}$	$1.0 \times 10^{-11}$	$1.0 \times 10^{-11}$
$L_2$ error	$3.0 \times 10^{-2}$	$1.7 \times 10^{-0}$	$9.4 \times 10^{-4}$	$5.3 \times 10^{-3}$	$3.9 \times 10^{-4}$	$1.7 \times 10^{-1}$	$1.7 \times 10^{-1}$	$1.7 \times 10^{-1}$

Table 6: Estimated errors for the model at  $\hat{\mu} = 2, \lambda = 0.7$ .

$\rho$	$\Upsilon_1(\rho)$	$\Upsilon_2(\rho)$	$\Upsilon_3(\rho)$	$\Upsilon_4(\rho)$	$\Upsilon_5(\rho)$	$\Upsilon_6(\rho)$	$\Upsilon_7(\rho)$	$\Upsilon_8(\rho)$
0.2	$4.4 \times 10^{-2}$	$1.7 \times 10^{-0}$	$7.9 \times 10^{-4}$	$3.5 \times 10^{-1}$	$8.8 \times 10^{-4}$	$4.3 \times 10^{-2}$	$4.5 \times 10^{-0}$	$3.2 \times 10^{-2}$
0.4	$7.2 \times 10^{-2}$	$1.6 \times 10^{-0}$	$1.2 \times 10^{-3}$	$5.0 \times 10^{-1}$	$1.6 \times 10^{-3}$	$1.6 \times 10^{-1}$	$2.6 \times 10^{-0}$	$1.8 \times 10^{-1}$
0.6	$6.5 \times 10^{-2}$	$1.6 \times 10^{-0}$	$1.1 \times 10^{-3}$	$5.8 \times 10^{-1}$	$1.5 \times 10^{-3}$	$2.6 \times 10^{-1}$	$9.6 \times 10^{-1}$	$2.8 \times 10^{-1}$
0.8	$1.0 \times 10^{-1}$	$1.7 \times 10^{-0}$	$5.4 \times 10^{-4}$	$6.1 \times 10^{-1}$	$8.0 \times 10^{-4}$	$1.9 \times 10^{-1}$	$2.1 \times 10^{-1}$	$1.6 \times 10^{-1}$
1.0	$2.0 \times 10^{-1}$	$1.7 \times 10^{-0}$	$3.4 \times 10^{-3}$	$5.8 \times 10^{-1}$	$5.3 \times 10^{-3}$	$1.7 \times 10^{-0}$	$2.9 \times 10^{-1}$	$1.7 \times 10^{-0}$
Max RE	$4.9 \times 10^{-1}$	$1.8 \times 10^{-0}$	$9.2 \times 10^{-3}$	$6.1 \times 10^{-1}$	$5.9 \times 10^{-3}$	$1.7 \times 10^{-0}$	$6.1 \times 10^{-0}$	$1.7 \times 10^{-0}$
Min RE	$3.2 \times 10^{-11}$	$1.6 \times 10^{-0}$	$5.5 \times 10^{-13}$	$7.5 \times 10^{-10}$	$9.5 \times 10^{-13}$	$6.1 \times 10^{-11}$	$7.2 \times 10^{-11}$	$3.2 \times 10^{-11}$
$L_2$ error	$1.2 \times 10^{-1}$	$1.7 \times 10^{-0}$	$2.2 \times 10^{-3}$	$5.1 \times 10^{-1}$	$2.3 \times 10^{-3}$	$4.5 \times 10^{-1}$	$3.0 \times 10^{-0}$	$4.4 \times 10^{-1}$

Table 7: Estimated errors for the model at  $\hat{\mu} = 3, \lambda = 0.7$ .

$\rho$	$\Upsilon_1(\rho)$	$\Upsilon_2(\rho)$	$\Upsilon_3(\rho)$	$\Upsilon_4(\rho)$	$\Upsilon_5(\rho)$	$\Upsilon_6(\rho)$	$\Upsilon_7(\rho)$	$\Upsilon_8(\rho)$
0.2	$1.4 \times 10^{-2}$	$1.6 \times 10^{-0}$	$5.9 \times 10^{-5}$	$6.2 \times 10^{-3}$	$2.7 \times 10^{-4}$	$2.1 \times 10^{-2}$	$1.9 \times 10^{-2}$	$1.9 \times 10^{-2}$
0.4	$1.8 \times 10^{-2}$	$1.6 \times 10^{-0}$	$3.9 \times 10^{-5}$	$7.6 \times 10^{-3}$	$3.9 \times 10^{-4}$	$6.3 \times 10^{-2}$	$6.0 \times 10^{-2}$	$6.0 \times 10^{-2}$
0.6	$1.5 \times 10^{-2}$	$1.7 \times 10^{-0}$	$1.3 \times 10^{-5}$	$6.3 \times 10^{-3}$	$3.6 \times 10^{-4}$	$9.0 \times 10^{-2}$	$8.7 \times 10^{-2}$	$8.7 \times 10^{-2}$
0.8	$9.0 \times 10^{-3}$	$1.7 \times 10^{-0}$	$1.5 \times 10^{-5}$	$3.4 \times 10^{-3}$	$2.1 \times 10^{-4}$	$7.1 \times 10^{-2}$	$6.9 \times 10^{-2}$	$6.9 \times 10^{-2}$
1.0	$9.1 \times 10^{-2}$	$1.6 \times 10^{-0}$	$8.8 \times 10^{-5}$	$3.4 \times 10^{-2}$	$2.2 \times 10^{-3}$	$9.1 \times 10^{-1}$	$8.9 \times 10^{-1}$	$8.9 \times 10^{-1}$
Max RE	$3.3 \times 10^{-1}$	$1.8 \times 10^{-0}$	$3.3 \times 10^{-3}$	$1.6 \times 10^{-1}$	$3.8 \times 10^{-3}$	$9.1 \times 10^{-1}$	$8.9 \times 10^{-1}$	$8.9 \times 10^{-1}$
Min RE	$4.4 \times 10^{-12}$	$1.6 \times 10^{-0}$	$4.9 \times 10^{-14}$	$2.3 \times 10^{-12}$	$5.2 \times 10^{-14}$	$6.3 \times 10^{-13}$	$1.8 \times 10^{-9}$	$1.8 \times 10^{-9}$
$L_2$ error	$5.6 \times 10^{-2}$	$1.7 \times 10^{-0}$	$4.2 \times 10^{-4}$	$2.6 \times 10^{-2}$	$9.3 \times 10^{-4}$	$1.9 \times 10^{-1}$	$1.9 \times 10^{-1}$	$1.9 \times 10^{-1}$

Table 8: Estimated errors for the model at  $\hat{\mu} = 2, \lambda = 0.5$ .

$\rho$	$Y_1(\rho)$	$Y_2(\rho)$	$Y_3(\rho)$	$Y_4(\rho)$	$Y_5(\rho)$	$Y_6(\rho)$	$Y_7(\rho)$	$Y_8(\rho)$
0.2	$4.1 \times 10^{-2}$	$1.7 \times 10^{-0}$	$8.6 \times 10^{-4}$	$4.0 \times 10^{-1}$	$3.0 \times 10^{-0}$	$1.2 \times 10^{-1}$	$1.1 \times 10^{-2}$	$1.0 \times 10^{-2}$
0.4	$6.1 \times 10^{-2}$	$1.6 \times 10^{-0}$	$1.2 \times 10^{-3}$	$5.1 \times 10^{-1}$	$1.6 \times 10^{-4}$	$2.1 \times 10^{-1}$	$3.1 \times 10^{-2}$	$3.8 \times 10^{-2}$
0.6	$5.2 \times 10^{-2}$	$1.6 \times 10^{-0}$	$1.1 \times 10^{-3}$	$5.4 \times 10^{-1}$	$2.3 \times 10^{-4}$	$2.7 \times 10^{-1}$	$3.9 \times 10^{-2}$	$4.8 \times 10^{-2}$
0.8	$2.4 \times 10^{-2}$	$1.7 \times 10^{-0}$	$5.1 \times 10^{-4}$	$5.4 \times 10^{-1}$	$1.4 \times 10^{-4}$	$2.4 \times 10^{-1}$	$2.5 \times 10^{-2}$	$1.5 \times 10^{-2}$
1.0	$1.5 \times 10^{-1}$	$1.7 \times 10^{-0}$	$3.1 \times 10^{-3}$	$5.0 \times 10^{-1}$	$1.0 \times 10^{-3}$	$1.1 \times 10^{-1}$	$1.9 \times 10^{-1}$	$1.9 \times 10^{-1}$
Max RE	$6.6 \times 10^{-1}$	$1.8 \times 10^{-0}$	$1.3 \times 10^{-2}$	$4.0 \times 10^{-1}$	$5.4 \times 10^{-3}$	$2.0 \times 10^{-1}$	$1.9 \times 10^{-1}$	$1.9 \times 10^{-1}$
Min RE	$2.2 \times 10^{-11}$	$1.6 \times 10^{-0}$	$4.6 \times 10^{-13}$	$1.4 \times 10^{-11}$	$6.3 \times 10^{-13}$	$8.7 \times 10^{-11}$	$1.1 \times 10^{-12}$	$1.1 \times 10^{-12}$
$L_2$ error	$1.2 \times 10^{-1}$	$1.7 \times 10^{-0}$	$2.6 \times 10^{-3}$	$7.8 \times 10^{-2}$	$6.3 \times 10^{-4}$	$6.3 \times 10^{-2}$	$5.6 \times 10^{-2}$	$5.6 \times 10^{-2}$

Table 9: Estimated errors for the model at  $\hat{\mu} = 3, \lambda = 0.5$ .

$\rho$	$Y_1(\rho)$	$Y_2(\rho)$	$Y_3(\rho)$	$Y_4(\rho)$	$Y_5(\rho)$	$Y_6(\rho)$	$Y_7(\rho)$	$Y_8(\rho)$
0.2	$1.5 \times 10^{-2}$	$1.6 \times 10^{-0}$	$2.6 \times 10^{-4}$	$9.2 \times 10^{-3}$	$5.9 \times 10^{-5}$	$4.2 \times 10^{-3}$	$5.0 \times 10^{-3}$	$5.0 \times 10^{-3}$
0.4	$1.8 \times 10^{-2}$	$1.6 \times 10^{-0}$	$2.9 \times 10^{-4}$	$1.0 \times 10^{-2}$	$1.1 \times 10^{-4}$	$1.5 \times 10^{-2}$	$1.6 \times 10^{-2}$	$1.6 \times 10^{-2}$
0.6	$1.5 \times 10^{-2}$	$1.7 \times 10^{-0}$	$2.3 \times 10^{-4}$	$8.9 \times 10^{-3}$	$1.1 \times 10^{-4}$	$2.2 \times 10^{-2}$	$2.2 \times 10^{-2}$	$2.2 \times 10^{-2}$
0.8	$8.2 \times 10^{-3}$	$1.7 \times 10^{-0}$	$1.2 \times 10^{-4}$	$4.8 \times 10^{-3}$	$7.1 \times 10^{-5}$	$1.6 \times 10^{-2}$	$1.6 \times 10^{-2}$	$1.6 \times 10^{-2}$
1.0	$8.0 \times 10^{-2}$	$1.6 \times 10^{-0}$	$1.1 \times 10^{-3}$	$4.7 \times 10^{-2}$	$7.7 \times 10^{-4}$	$2.0 \times 10^{-1}$	$2.0 \times 10^{-1}$	$2.0 \times 10^{-1}$
Max RE	$5.4 \times 10^{-1}$	$1.8 \times 10^{-0}$	$1.0 \times 10^{-2}$	$3.2 \times 10^{-1}$	$7.7 \times 10^{-4}$	$2.0 \times 10^{-1}$	$2.0 \times 10^{-1}$	$2.0 \times 10^{-1}$
Min RE	$6.0 \times 10^{-12}$	$1.6 \times 10^{-0}$	$5.4 \times 10^{-13}$	$3.6 \times 10^{-12}$	$1.2 \times 10^{-13}$	$2.0 \times 10^{-12}$	$4.7 \times 10^{-5}$	$4.7 \times 10^{-5}$
$L_2$ error	$7.2 \times 10^{-2}$	$1.7 \times 10^{-0}$	$1.3 \times 10^{-3}$	$4.3 \times 10^{-2}$	$2.1 \times 10^{-3}$	$4.4 \times 10^{-2}$	$4.4 \times 10^{-2}$	$4.4 \times 10^{-2}$

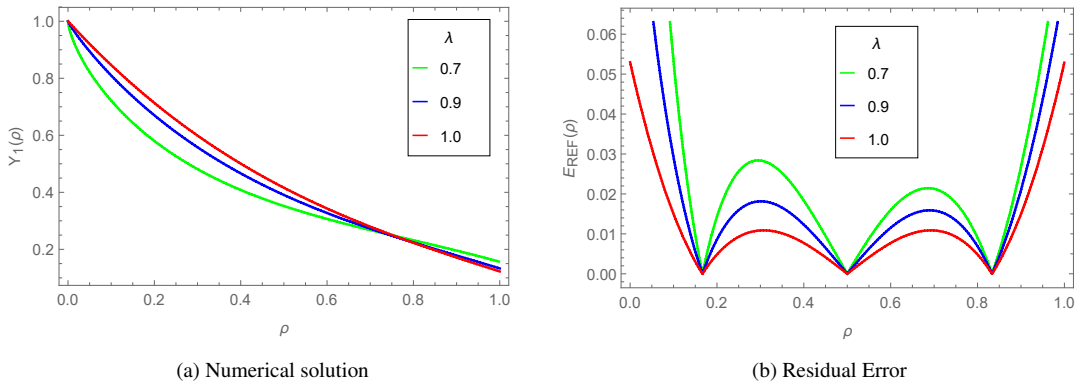


Figure 2: Behavior of  $Y_1(\rho)$  with fractional derivative.

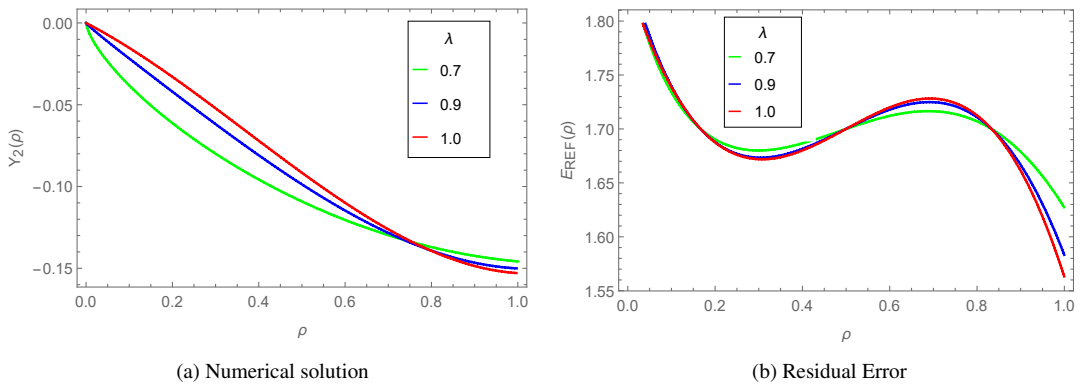


Figure 3: Behavior of  $Y_2(\rho)$  with fractional derivative.

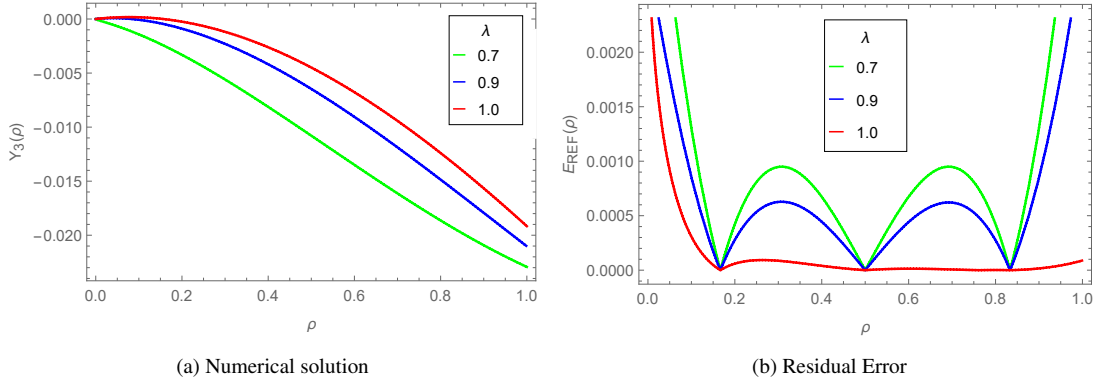


Figure 4: Behavior of  $Y_3(\rho)$  with fractional derivative.

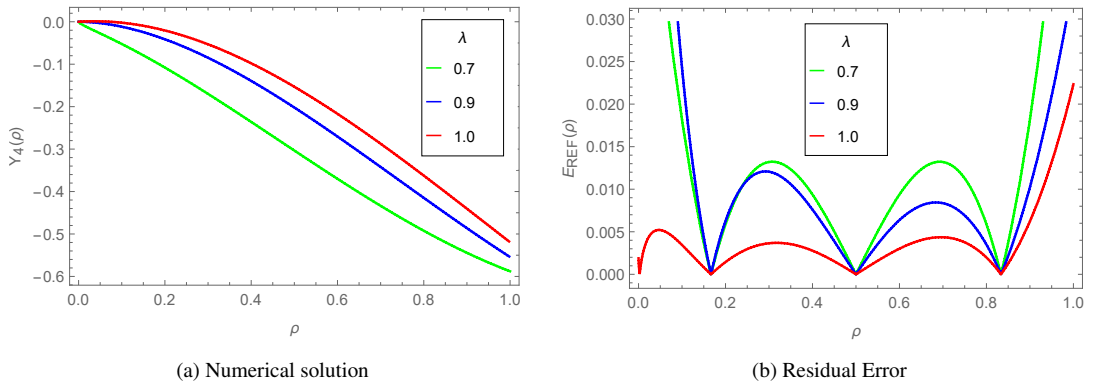


Figure 5: Behavior of  $Y_4(\rho)$  with fractional derivative.

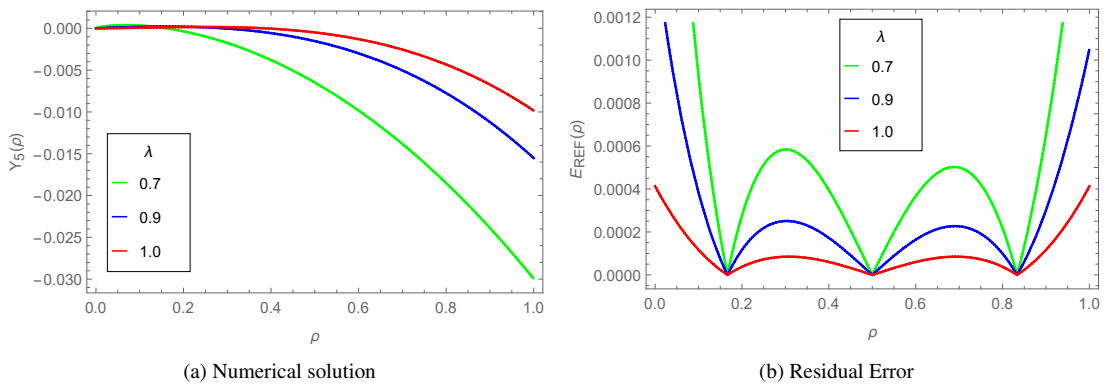


Figure 6: Behavior of  $Y_5(\rho)$  with fractional derivative.

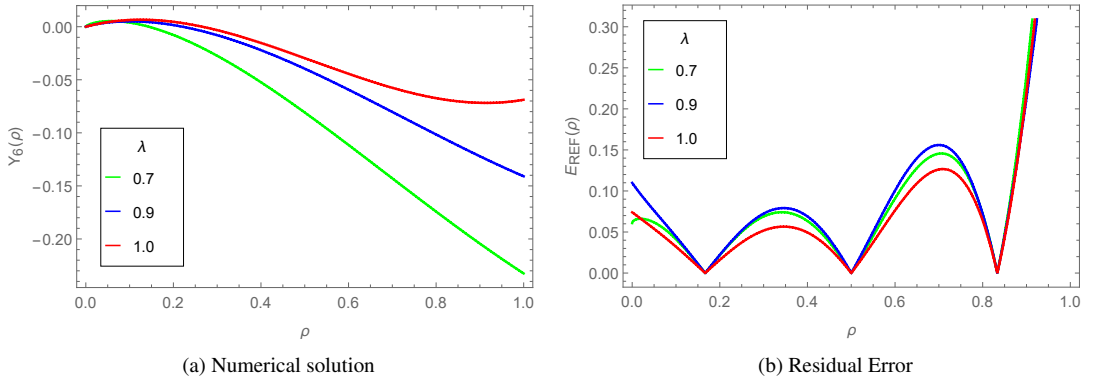


Figure 7: Behavior of  $Y_6(\rho)$  with fractional derivative.

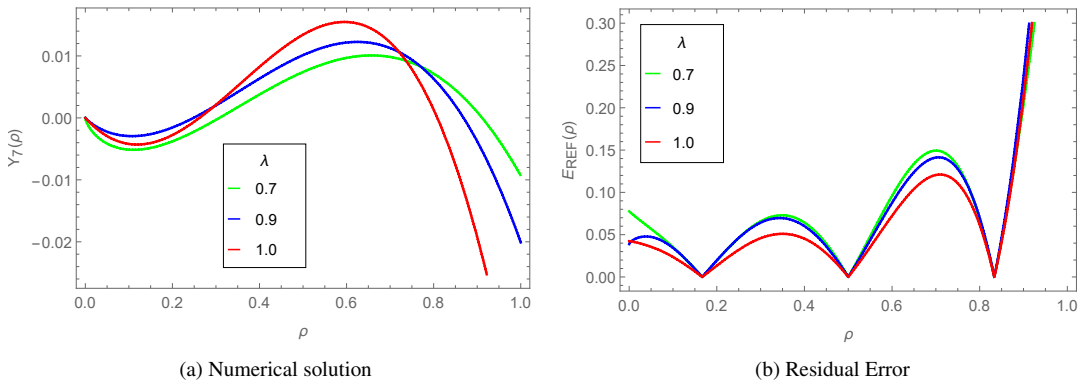


Figure 8: Behavior of  $Y_7(\rho)$  with fractional derivative.

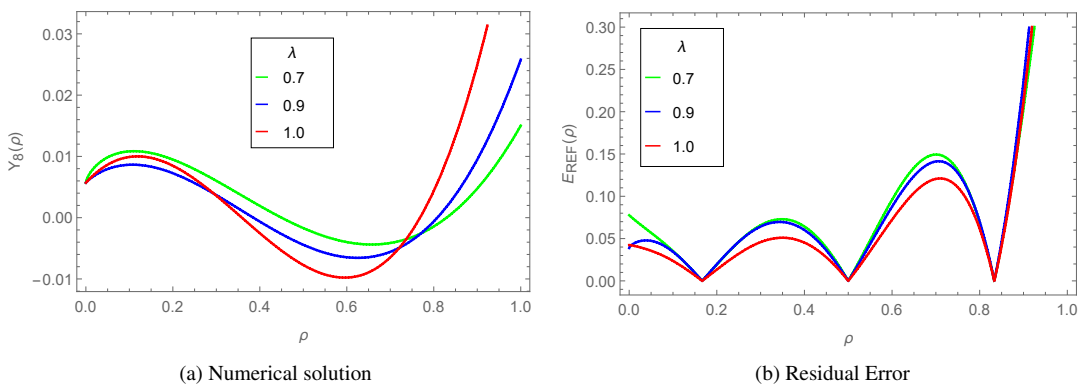


Figure 9: Behavior of  $Y_8(\rho)$  with fractional derivative.

## 7 Conclusion

The integration of USWs with the Caputo fractional derivative provides a robust numerical framework for solving a fractional nonlinear HIRES problem arising in chemical kinetics. This approach combines the localization and approximation power of wavelets with the flexibility of fractional calculus, offering a promising method for dealing with stiff systems. The solutions have been achieved efficiently within a limited timeframe, demonstrating the actual behavior of chemical kinetics problems. This work shows several dynamical behaviors in terms of graphs for any arbitrary order. With these graphical representations, we can see that arbitrary order derivatives significantly affect fractional HIRES problem. Therefore, we believe that the present study will shed light on future investigations and applications of the complex Caputo fractional system.

## References

- [1] P. L. Butzer and U. Westphal, An introduction to fractional calculus. In Applications of Fractional Calculus in Physics. *World Scientific* 1-85 (2000).
- [2] K. S. Miller and B. Ross, An Introduction to the Fractional Calculus and Fractional Differential Equations. *Wiley: New York, USA* (1993).
- [3] M. Caputo and M. Fabrizio, On the Singular Kernels for Fractional Derivatives. Some Applications to Partial Differential Equations. *Progr. Fract. Differ. Appl.* **7**, 79-82 (2021).
- [4] W. M. Abd-Elhameed, H. M. Ahmed, M. A. Zaky and R. M. Hafez, A new shifted generalized Chebyshev approach for multi-dimensional sinh-Gordon equation. *Phys. Scr.* **99**, 095269 (2024).
- [5] W. M. Abd-Elhameed, A. M. Al-Sady, O. M. Alqubori and A. G. Atta, Numerical treatment of the fractional Rayleigh-Stokes problem using some orthogonal combinations of Chebyshev polynomials. *AIMS Mathematics* **9(9)**, 25457-25481 (2024).
- [6] M. H. Alharbi, A. F. Abu Sunayh, A. G. Atta and W. M. Abd-Elhameed, Novel Approach by Shifted Fibonacci Polynomials for Solving the Fractional Burgers Equation. *Fractal Fract.* **8**, 427 (2024).
- [7] W. Abd-Elhameed, M. Al-Harbi and A. Atta, New convolved Fibonacci collocation procedure for the Fitzhugh-Nagumo non-linear equation. *Nonlinear Engineering* **13(1)**, 20220332 (2024).
- [8] N. T. Linh and B. T. N. Han, A nonlinear fractional Pantograph equation with a state-dependent non-local condition. *Palestine Journal of Mathematics* **12(4)**, 204-214 (2023).
- [9] B. Roy and S. N. Bora, Impulsive differential equations with Erdélyi-Kober boundary conditions and fractional derivatives of Caputo type. *Palestine Journal of Mathematics* **12(3)**, 133-150 (2023).
- [10] A. Rayal, P. Bisht, S. Giri, P. A. Patel and M. Prajapati, Dynamical analysis and numerical treatment of pond pollution model endowed with Caputo fractional derivative using effective wavelets technique. *International Journal of Dynamics and Control* 1-14 (2024).
- [11] M. Ferhat and T. Blouhi, Existence for coupled Random system fractional order functional differential with infinite delay. *Palestine Journal of Mathematics* **13(1)**, 232-241 (2024).
- [12] C. Dhivya and M. K. Panthangi, Different order B-splines with the Galerkin Method for a coupled system of nonlinear Boundary value problems. *Palestine Journal of Mathematics* **13(3)**, 82-95 (2024).
- [13] W. M. Abd-Elhameed and H. M. Ahmed, Spectral solutions for the time-fractional heat differential equation through a novel unified sequence of Chebyshev polynomials. *AIMS Mathematics* **9(1)**, 2137-2166 (2024).
- [14] G. Scholz and F. Scholz, First-order differential equations in chemistry, *Chem Texts* **1**, (2015).
- [15] G. Craciun, M. D. Johnston, G. Szederkenyi, E. Tonello and P. Y. Yu, Realizations of kinetic differential equations. *Math. Biosci. Eng.* **17**, 862-892 (2020).
- [16] A. Akgul, H. Sarbaz and A. Khoshnaw, Application of fractional derivative on non-linear biochemical reaction models. *Int. J. Intell. Net.* **1**, 52-58 (2020).
- [17] E. Schafer, A new approach to explain the high irradiance responses of photomorphogenesis on the basis of phytochrome. *J. Math. Biology* **2**, 41-56 (1975).
- [18] S. Amat, M. J. Legaz and J. iz-Alvarez, On a variational method for stiff differential equations arising from chemistry kinetics. *Mathematics* **7**, 459 (2019).
- [19] H. Soomro, N. Zainuddin, H. Daud, J. Sunday, N. Jamaludin, A. Abdullah, M. Apriyanto and E. A. Kadir, Variable Step Block Hybrid Method for Stiff Chemical Kinetics Problems. *Appl. Sci.* **12**, 4484 (2022).
- [20] H. Wu, P. C. Ma and M. Ihme, Efficient time-stepping techniques for simulating turbulent reactive flows with stiff chemistry. *Computer Physics Communications* **243**, 81-96 (2019).

- [21] Y. Skwame, J. Sabo and M. Mathew, The treatment of second order ordinary differential equations using equidistant one-step block hybrid. *Asian Journal of Probability and Statistics* **5**(3), 1-9 (2019).
- [22] R. D. Ambrosio, M. Ferro and B. Paternoster, Trigonometrically fitted two-step hybrid methods for special second order ordinary differential equations. *Mathematics and Computers in Simulation* **81**(5), 1068-1084 (2011).
- [23] E. K. Pushpam and D. P. Dhayabaran, An Application of STWS Technique in Solving Stiff Non-linear System: High Irradiance Responses (HIRES) of Photomorphogenesis. *Recent Research in Science and Technology* **3**, 47-53 (2011).
- [24] M. Aslam, M. Farman, H. Ahmad, T. N. Gia, A. Ahmad and S. Askar, Fractal fractional derivative on chemistry kinetics hires problem. *AIMS Math.* **7**, 1155-1184 (2022).
- [25] C. K. Chui, *An Introduction to Wavelets*. Academic Press, San Diego, CA (1992).
- [26] S. Mallat, *A Wavelet Tour of Signal Processing: The Sparse Way*, Elsevier Science (2008).
- [27] L. Debnath, *Wavelets Transform and Their Applications*. Birkhauser, Boston (2002).
- [28] A. B. Deshi and G. A. Gudodagi, The numerical solution of hyperbolic differential equations using Wavelet lifting scheme. *Palestine Journal of Mathematics* **12**(3), 7-14 (2023).
- [29] A. Rayal, An effective Taylor wavelets basis for the evaluation of numerical differentiations. *Palestine Journal of Mathematics* **12**(1), 551-568 (2023).
- [30] A. Rayal, M. Anand and V. K. Srivastava, Application of Fractional Modified Taylor Wavelets in the Dynamical Analysis of Fractional Electrical Circuits under Generalized Caputo Fractional Derivative. *Physica Scripta* (2024). 10.1088/1402-4896/ad8701
- [31] A. Rayal and S. R. Verma, An approximate wavelets solution to the class of variational problems with fractional order. *Journal of Applied Mathematics and Computing* **65**, 735-769 (2020).
- [32] A. Rayal and S. R. Verma, Numerical analysis of pantograph differential equation of the stretched type associated with fractal-fractional derivatives via fractional order Legendre wavelets. *Chaos, Solitons Fractals* **139**(1), 110076 (2020).
- [33] A. Rayal and S. R. Verma, Two-dimensional Gegenbauer wavelets for the numerical solution of tempered fractional model of the nonlinear Klein-Gordon equation. *Applied Numerical Mathematics* **174**, 191-220 (2022).
- [34] A. Rayal, B. P. Joshi, M. Pandey and D. F. M. Torres, Numerical Investigation of the Fractional Oscillation Equations under the Context of Variable Order Caputo Fractional Derivative via Fractional Order Bernstein Wavelets. *Mathematics* **11**, 2503 (2023).
- [35] A. Rayal, M. Anand, K. Chauhan and Prinsa. An Overview of Mamadu-Njoseh wavelets and its properties for numerical computations. *Uttaranchal Journal of Applied and Life Sciences*, Uttaranchal University **4**(1), 1-8 (2023).
- [36] A. Rayal and S. R. Verma, Numerical study of variational problems of moving or fixed boundary conditions by Muntz wavelets. *Journal of Vibration and Control* **28**, 1-16 (2020).
- [37] A. Rayal, Muntz Wavelets Solution for the Polytropic Lane-Emden Differential Equation Involved with Conformable Type Fractional Derivative. *Int. J. Appl. Comput. Math.* **9**, 50 (2023).
- [38] A. Rayal, P. A. Patel, S. Giri and P. Joshi, A Comparative study of a class of Linear and Nonlinear Pantograph Differential Equations via different orthogonal polynomial Wavelets, *Malaysian Journal of Science* **43**(2), 75-95 (2024).
- [39] A. Rayal and P. Joshi, A comprehensive review on fractional operators, wavelets, and their applications. *Redshine Archive* **11**(4), 380-387 (2024).
- [40] I. Celik, Generalization of Gegenbauer Wavelet Collocation Method to the Generalized Kuramoto-Sivashinsky Equation. *Int. J. Appl. Comput. Math.* **4**, 111 (2018).
- [41] N. Ozdemir and A. Secer, A numerical algorithm based on ultraspherical wavelets for solution of linear and nonlinear Klein Gordon equations. *Sigma Journal of Engineering and Natural Sciences* **38**(3), 1307-1319 (2020).
- [42] M. Mulimani and K. Srinivasa, A novel approach for Benjamin-Bona-Mahony equation via ultraspherical wavelets collocation method. *International Journal of Mathematics and Computer in Engineering* **2**, 39-52 (2024).
- [43] W. M. Abd-Elhameed and Y. H. Youssri, New Spectral Solutions of Multi-Term Fractional-Order Initial Value Problems With Error Analysis. *Computer Modeling in Engineering & Sciences* **105**(5), 375-398 (2015).

**Author information**

<sup>1\*</sup>Ashish Rayal, <sup>2</sup>Jasmeet Kaur, <sup>3</sup>Vikash Verma, <sup>4</sup>Priya Dogra, <sup>1,2,3,4</sup>Department of Mathematics, School of Applied & Life Sciences, Uttarakhand University, Dehradun-248007, Uttarakhand, India.

E-mail: \*ashish1989rayal@gmail.com; \*Corresponding author

Received: 2024-07-24

Accepted: 2024-10-25